4. Result and discussion:

4.1 Coating characterization:

The microstructure of the coating was studied with the help of scanning electron microscope. The surface of the coating showed in the microstructure in which the splat of the sprayed material does not seem to form a continuous layer but at the cross section, it observed the coating was more homogeneous and regular (figure 25a).

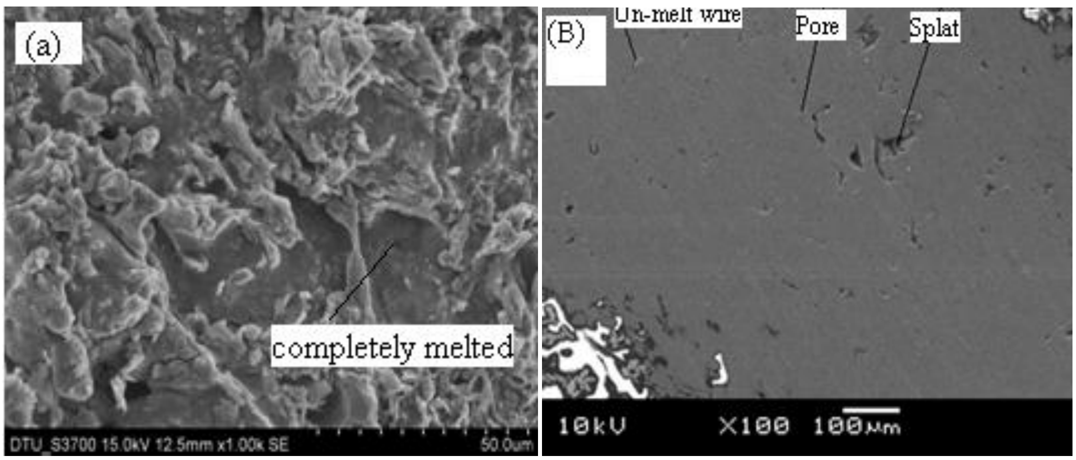

Figure 25. (a) Top view of sprayed coating (b) Cross section of thermal spray coating

The inner side material deposited in continuous layer because the two wires electric spray coating provides the wire material gets melted completely, and the porosity and the blow holes were negligible (figure 25b) [15]. Some small particles of the unmelted wire were also observed.

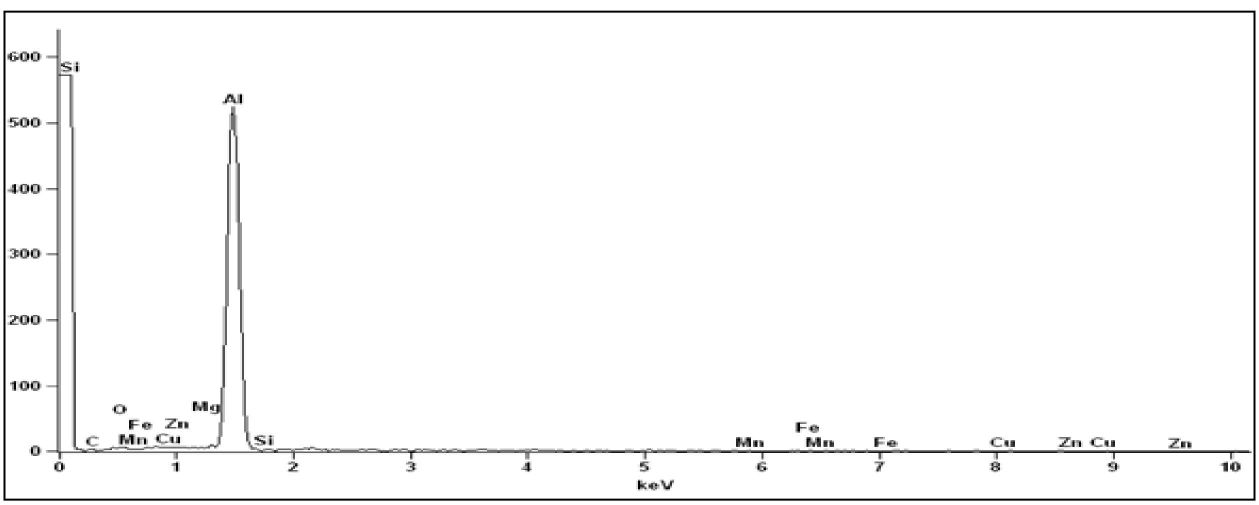

Figure 26. EDS analysis of thermal spray coating

The EDS analysis of the coating material was analyzed in the thermo EDS analyzer, and it was found that the coating material was an alloy of the aluminum 98.76%, magnesium 0.82% and manganese 0.43% (figure 26). As in the coating material aluminum was the major constituents, when we sprayed the coating the coatings get oxidized during the spraying process. Some negligible amount of the copper, zinc and the iron were also present in the aluminum in the form of impurity [57]. The coating of aluminum has a property to form an oxide layer over it. It protects the aluminum from the atmosphere and also from the chemical environment [4].

Element Line	**Net Counts**	**ZAF**	**Weight %**	**Weight % Error**	**Atom %**	**Atom % Error**	**Compound%**
C K	18	10.950	3.43	+/- 1.14	7.34	+/- 2.45	3.43
O K	31	3.037	2.38	+/- 0.62	3.83	+/- 0.99	2.38
Mg K	0	1.009	0.00	---	0.00	+/- 0.00	0.00
Al K	5710	1.048	92.33	+/- 1.25	88.06	+/- 1.19	92.33
Si K	0	2.169	0.00	---	0.00	+/- 0.00	0.00
Si L	0	0.000	---	---	---	---	---
Mn K	0	1.185	0.00	---	0.00	+/- 0.00	0.00
Mn L	0	0.000	---	---	---	---	---
Fe K	3	1.168	0.32	+/- 0.76	0.15	+/- 0.35	0.32
Fe L	0	0.000	---	---	---	---	---
Cu K	2	1.223	0.57	+/- 1.70	0.23	+/- 0.69	0.57
Cu L	0	0.000	---	---	---	---	---
Zn K	3	1.228	0.97	+/- 1.93	0.38	+/- 0.76	0.97
Zn L	0	0.000	---	---	---	---	---
Total			100.00		100.00		100.00

Table 3.Quantitative table of EDS analysis of thermal spray

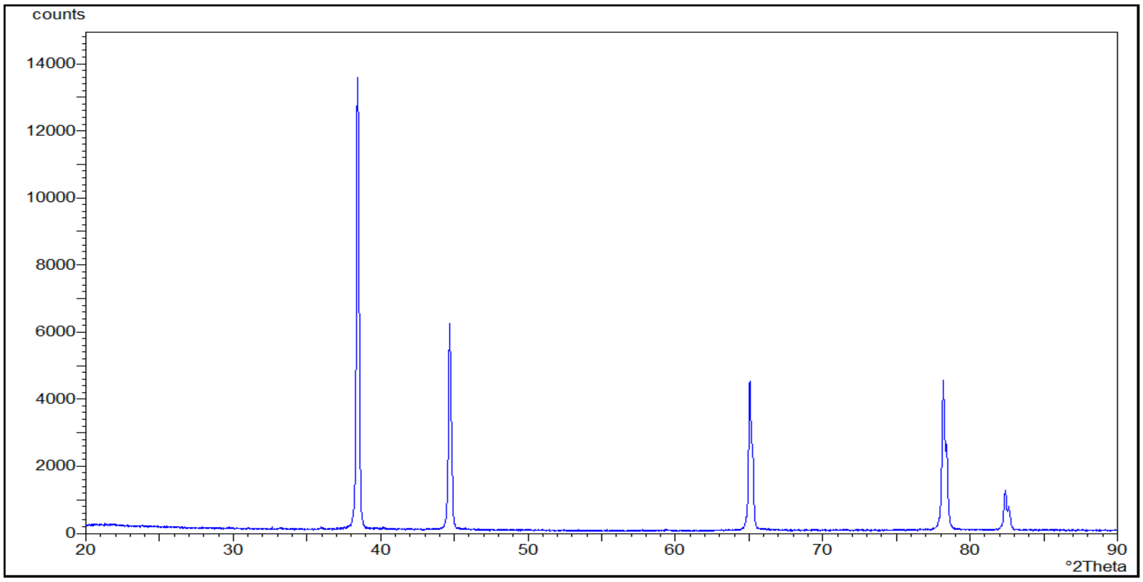

Figure 27. XRD peaks for the thermal spray coating

The XRD of the coating material was done to find the change in the phase of coating. For that purpose the XRD peaks of the coating material was analyzed (figure 27), and it was found that the higest intensity peaks is of α-Al_2O_3, however some γ- Al_2O_3 were also present in the coating. If the magnesium contents exceeds 3-4%, there is atendency for the β-phase, Mg_5Al_8, to precipitate in slip bands and grain boundaries which may lead to intergranular attack and stress-corrosion cracking in corrosive conditions [58]. The other peaks observeed were magnesium, manganese and the impurity materials.

4.2. Wear rate of thermal spray coating:

4.2.1. Wear rate with brass pin:

The wear rate of the coating in terms of mass loss per 74.4 m sliding distance was calculated. To find the wear rate of the coating the two variables were chosen as already described that are load and sliding speed. The load was chosen as 29.9, 44.1 and 58.8 N and the sliding speed was chosen as 150, 200, and 250 rpm. By using these two variables and three levels a set of ANOVA was designed. The ANOVA model gives the F-value and compare with the standard table to decide the model variables are significant or not. In this case, the Model F-value is 12652.07 which implies that the model is significant. There is only a 0.01% chance that the "Model F-Value" is large that could occur due to noise. This noise may be due to some hard particles in the coating. Values of probability are greater than F value and less than 0.0500 indicate model terms are significant. In this case load, sliding speed and their interaction are significant model terms. If the probability values greater than 0.1000, it indicate that the model terms are not significant.

Final Equation in Terms of Coded Factors:

Mass Loss = + 0.024 + 2.514 $*10^{-4}$ * load - 7.868 * 10^{-4} * load^2 + 3.108 * 10^{-3} * sliding speed + 4.417 * 10^{-4} * sliding speed^2 + 2.801 $*10^{-5}$ * load *sliding speed - 5.256 * 10^{-4} * load^2 * sliding speed + 2.897 * 10^{-6} * load * sliding speed^2 - 1.693 $*10^{-4}$ * load^2 * sliding speed^2.

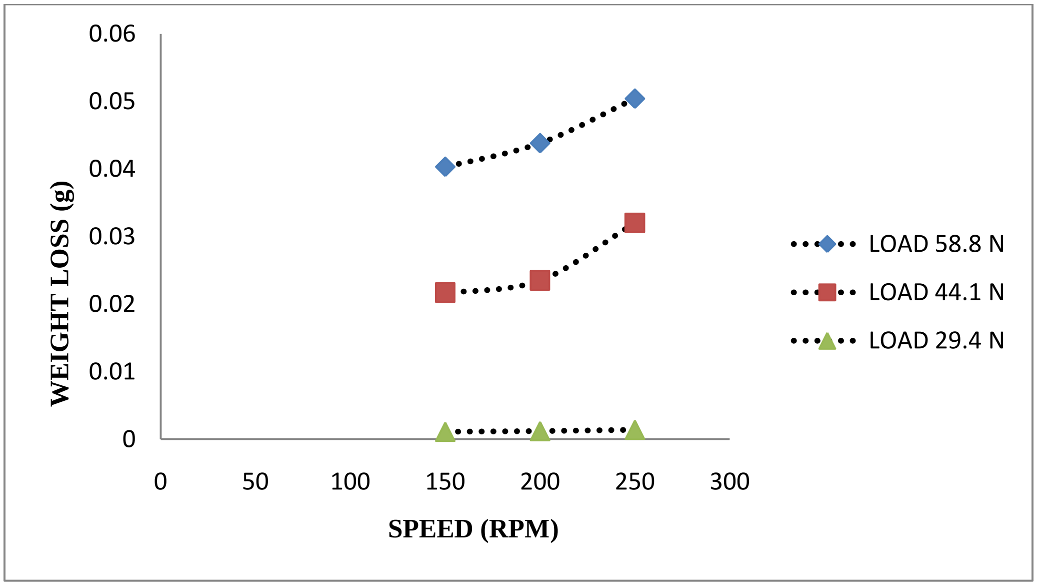

Figure 28. Mass loss of coating with brass pin at various loading and sliding conditions

Figure 28 shows the variation of the wear rate of the coating at different loads as well as sliding speeds. The wear rate of the coating at 150 rpm speed, and 29.9 N load was found to be 0.0011 g. The wear rate was increased to 0.0217 g when the load was increased to 44.1 N. The wear rate at 58.8 N load was further increased to 0.0403 g. The wear rate of the coating at 200 rpm speed and 29.9 N load was found to be 0.0012 g. When the load was further increased to 44.1 at same rpm; the wear rate was 0.0235 g. The wear rate was further found to increase to 0.0438 g at the load of 58.8 N. The wear rate of the coating at 250 rpm speed and 29.9 N load was calculated as 0.0014 g. The wear rate further increased to 0.0320 g at the load of 44.1 N and to 0.0504 g, at a load of 58.8 N, under the same sliding speed.

The wear rate at low load and low sliding speed was found to be very low. The wear rate of coating increased to a lesser degree with increase of the sliding speed at lower loads. The wear rate increased when the sliding speed of the disc was increased. The wear rate was also found to increase with increased load [8,41]. The wear rate was increased more with increased load as compared to increased sliding speed. It can be concluded that at lower sliding speed and lower load the wear is caused by adhesion and very less abrasion. When either one of two surfaces of tribo-elements in sliding or rolling contact has thin soft surface layer that can be partly transferred to the counter surface by adhesion relative displacement takes place at the interface between the surfaces of coating and transfer layer with smaller shear strength of the soft material than that of the underlying element material [30]. This was further explained by Subramanian et al. [52] that during wear test of aluminum alloy with a copper pin, a tribolayer of aluminum alloy forms on the copper pin. This tribolayer was formed at low load and low sliding velocity. The wear rate of the coating was decreased by the tribolayer. The brass pin at low speed and high load showed high deformation and low wear rate because the micro hardness of coating used was 58 Hv at 5 g load; which is very less as compared to hardness of the brass. A.P. Sannino et al. [31] found that the wear rate also depends on the sliding speed; it is low at low speed and increases with increasing speed. The similar behavior that the wear rate increases with increase in load has also been reported by Koji Kato et al. [51].

4.2.2 Wear rate with medium carbon steel pin:

Wear rate of the coating with medium carbon steel under similar loading and sliding conditions were calculated as described earlier. By using these two variables and three levels a set of ANOVA was designed as in the last case with design expert 8.0.1 software. The Model F-value of 974.55 implies the model is significant. In this case load, sliding speed and interaction effect are significant model terms.

Final Equation in Terms of Significant Coded Factors:

Mass Loss = $+0.059 + 1.794 * 10^{-4} * \text{load} + 2.230 * 10^{-4} * \text{load}^2 + 0.012 * \text{sliding speed} + 1.483 * 10^{-3} * \text{sliding speed}^2 + 9.959 * 10^{-5} * \text{load} * \text{sliding speed} + 1.933 * 10^{-3} * \text{load}^2 * \text{sliding speed} + 1.390 * 10^{-5} * \text{load} * \text{sliding speed}^2 + 3.044 * 10^{-4} * \text{load}^2 * \text{sliding speed}^2$.

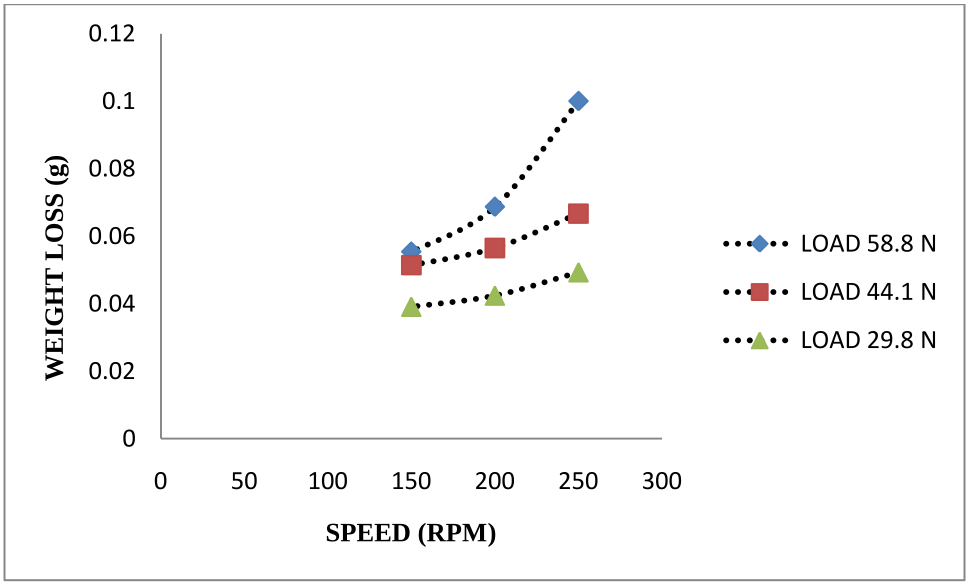

Figure 29. Mass loss of the coating with medium carbon steel pin coating at various sliding and loading conditions

Figure 29 shows the variation of the wear rate of the coating at different load and sliding speed with medium carbon steel pin. The wear rate of the coating at 150 rpm speed, and 29.9 N load was calculated as 0.0391 g. The wear rate increased to 0.0514 g when the load was increased to 44.1 N. The wear rate at 58.8 N load further increased to 0.0554 g. The wear rate of the coating at 200 rpm speed, and 29.9 N load was 0.0424 g. When the load was further increased to 44.1 at same rpm; the wear rate increased to 0.0565 g. The wear rate further increased to 0.0687 g at the load of 58.8 N. The wear rate of the coating at 250 rpm speed and 29.9 N load was calculated as 0.0493 g. The wear rate increased to 0.0667 g at the load of 44.1 N. The wear rate was further increased to 0.1 g, at a load of 58.8 N, under same sliding speed.

The wear rate of the coating with medium carbon steel pin was found to be higher than the wear rate of the coating with brass pin. W. Maa et al. [51] showed that the wear behaviour of different material is different with different counter materials. The wear rate of the coating increased slightly with increased in the sliding speed at low load. But at high load the wear rate increased to a higher value at the increased sliding speed. It case of medium carbon steel pin the material gets eroded fast so the coefficient of friction and the wear rate were found to be more [51,54].

The wear rate of the coating with medium carbon steel pin was higher as the steel pin is much harder compared to the aluminum alloy coating, and the wear mechanism was mainly due to micro cutting.

4.2.3. Wear rate with high carbon steel pin:

The wear of the coating was also analyzed with high carbon steel pin under the same loading and sliding conditions. The ANOVA of these two variables were also designed to find the significance of the two variables and their interactions. The Model F-value of 1256.08 implies the model is significant. The significant model terms are load, sliding speed and their interaction effects.

Final Equation in Terms of significant Coded Factors:

Mass Loss=+0.065 + 1.638 $*10^{-4}$ * load + 7.193 $*10^{-4}$ * load^2 + 0.019 * sliding speed - 3.153 * 10^{-3} * sliding speed^2 + 2.970 $*10^{-5}$ * load * sliding speed + 2.135 $*10^{-3}$ * load^2 * sliding speed - 1.177 $*10^{-6}$ * load * sliding speed^2 + 1.221 $*10^{-4}$ * load^2 * sliding speed^2.

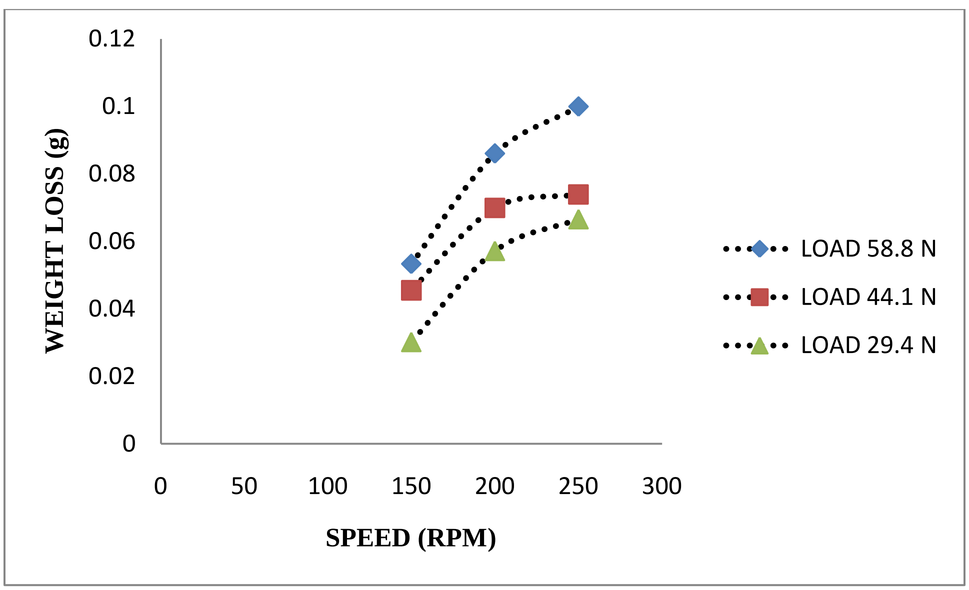

Figure 30. Mass loss of the coating with high carbon steel pin coating at various sliding and loading conditions

Figure 30 shows the variation of the wear rate of the coating at different loading and sliding speed with high carbon steel pin. The wear rate of the coating at 150 rpm speed and 29.9 N load was 0.0302 g. The wear rate increased to 0.0455 g when the load was increased to 44.1 N. The wear rate at 58.8 N load further increased to 0.0533 g. The wear rate of the coating at 200 rpm speed, and 29.9 N load was 0.0572 g. When the load was further increased to 44.1 at same rpm the wear rate was 0.0699 g. The wear rate further increased to 0.0860 g at the load of 58.8 N. The wear rate of the coating at 250 rpm speed and 29.9 N load found to 0.0666 g. The wear rate was increased to 0.0739 g at the load of 44.1 N. The wear rate was further increased to 0.0999 g at a load of 58.8 N under same sliding speed.

It is clear from Figure 40 that the wear rate of the coating with high carbon steel was low at low load and low sliding speed [41], but as the sliding speed was increased to some moderate value the wear rate increased abruptly. However, when the sliding speed was further increased then the increase in the wear rate was small. The wear rate also increased with the increased value of the load [8]. At low speed the value of wear rate increased with load, but the increment was very less. However, at higher sliding speed the value of wear rate increased abruptly with increased loading conditions. It was found that the wear rate of the coating was more than that with the brass pin and the medium carbon pin [51, 54]. It was concluded that at the lower loads, the coating wear was mainly due to adhesion and deformation, and other modes of wear did not observed as reported earlier [55].

4.3. Coefficient of friction of the coating:

4.3.1. Coefficient of friction of the coating with brass pin:

The co-efficient of friction of the coating at three loads (29.9, 44.1 and 58.8 N) and three sliding conditions (150, 200 and 250 rpm) were analysed. A statistical ANOVA was designed based on two variables and three level of each variable in design expert 8.0.1 software. The Model F-value of 128.14 implies the model is significant. In this case load and sliding speed and interaction effect are significant model terms.

Final Equation in Terms of Significant Coded Factors:

Co-efficient of friction = + 0.74 - 4.945 $*10^{-4}$ * load + 2.498 * 10^{-3} * $load^2$ - 0.092 * sliding speed + 0.012 * sliding $speed^2$ - 1.411 * 10^{-5} * load * sliding speed + 0.017 * $load^2$ * sliding speed + 8.373 $*10^{-6}$ * load * sliding $speed^2$ - 8.913 $*10^{-4}$ * $load^2$* sliding $speed^2$.

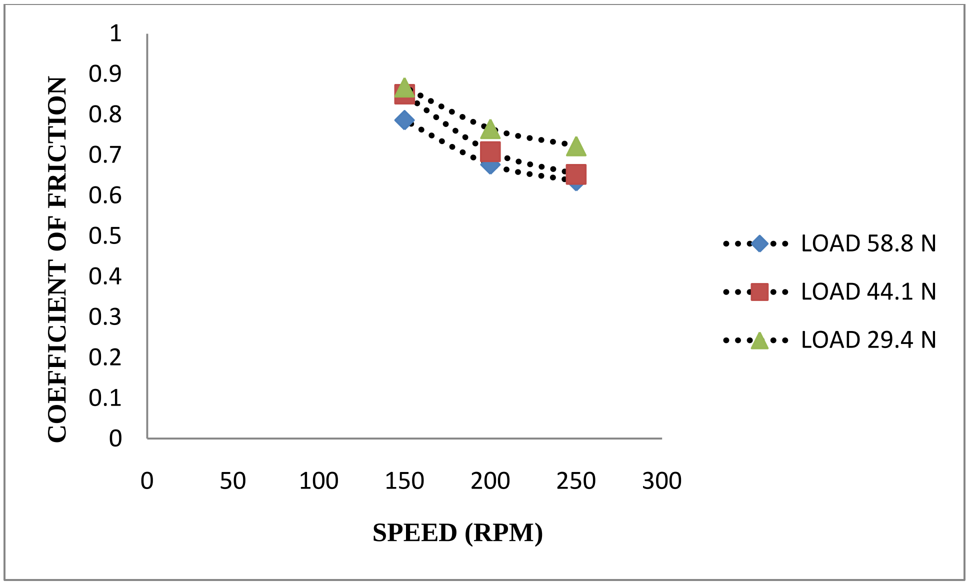

Figure 31. Variation of coefficient of friction with brass pin at various loading and sliding conditions

Figure 31 shows the variation of the co-efficient of friction of the coating at different loading and sliding condition with brass pin. The coefficient of friction of the coating at 29.9 N load and 150 rpm was calculated as 0.8678. The coefficient of friction decreased to 0.7653, at a load of 44.1 N at the same speed. When the load was increased to 58.8 N at the same sliding speed the co-efficient of friction was further decreased to 0.7866. The co-efficient of friction of the coating at 200 rpm speed and 29.9 N load was found to be 0.7653. When the load was increased to 44.1 N at the same sliding speed, the co-efficient of friction decreased to 0.7086. It further decreased to 0.6765, when the load was increased to 58.8 at the same sliding speed. The co-efficient of friction at 250 rpm speed and 29.9 N load was found to be 0.7228. The co-efficient of friction was found decrease further when the load increased to 44.1 N and 58.8 N respectively at the same sliding speed.

The coefficient of friction of the coating decreased, when the sliding speed was increased. The decrease in co-efficient was more significant with increase in sliding speed. A. Edrisy et al. [53] has earlier reported that at high sliding speed and high load the coefficient of friction was low. However, the variation in the co-efficient of friction with variation in load was very less which is contrary to Binshi Xu et al. [9] as in general they found that the coefficient of friction of aluminum alloy decreases with an increase in load. This may be because the brass pin is a soft material, and it deformed during the wear test.

4.3.2. Coefficient of friction of the coating with medium carbon steel:

The co-efficient of friction of coating with medium carbon steel pin was analyzed under similar loading and sliding conditions, and a design of experiment was set to do the ANOVA of the process variables. The Model F-value of 1023.37 implies the model is significant.

Final Equation in Terms of Significant Coded Factors:

Co-efficient of friction = + 0.75 - 4.667 * 10^{-4} * load - 2.588 * 10^{-3} * load^2 - 0.038 * sliding speed - 3.333 *10^{-5} * sliding speed^2 + 1.908 * 10^{-4} * load * sliding speed - 6.334 * 10^{-3} * load^2 * sliding speed - 1.058 *10^{-4} * load * sliding speed^2 + 6.088 * 10^{-4} * load^2 *sliding speed^2.

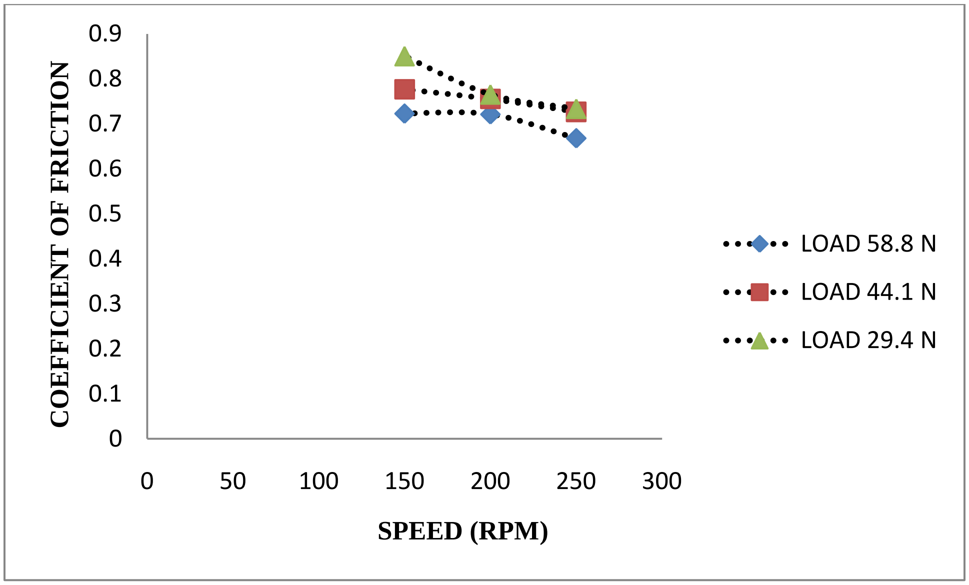

Figure 32. Variation of coefficient of friction with medium carbon steel pin at various loading and sliding conditions

Figure 32 shows the variation of the co-efficient of friction of the coating at different loading and sliding condition with medium carbon steel pin. The coefficient of friction of the coating at 29.9 N load and 150 rpm was found to be 0.8503. The coefficient of friction was found decrease to 0.7769 at a load of 44.1 N at the same 150 rpm speed. When the load was increased to 58.8 N at the same sliding speed the co-efficient of friction further decreased to 0.7228. The co-efficient of friction of the coating at 200 rpm speed and 29.9 N load was 0.7653. With the increased of load to 44.1 N at the same sliding speed it again decreased to 0.7553. It further decreased to 0.7212, when the load was increased to 58.8 at the same sliding speed. The co-efficient of friction at 250 rpm speed and 29.9 N load was 0.7336. It decreased to 0.7266, when the load was increased to 44.1, at the same sliding speed. The co-efficient of friction further decreased to 0.6677 at 58.8 N load and same 250 rpm sliding speed.

The Coating showed higher co-efficient of friction with medium carbon steel pin as compared to brass pin. The coefficient of friction in case of the medium carbon steel pin was higher than in case of brass pin [51,54]. The coefficient of friction was decreased with increased loading conditions. It was decreased may be due to reason that at increased load, the wear rate was more, that's why the direct rubbing was less. And it showed less coefficient of friction. The co-efficient of friction at 29.9 N load and 44.1 N load was almost same at 200, and 250 rpm speed. The wear rate was also decreased with increase in sliding speed. The co efficient of friction is low when the load is high and sliding speed is high [12,53]. The Binshi Xu et al. [9] found that the coefficient of friction of aluminum alloy decreases with an increase in load.

4.3.3. Coefficient of friction of the coating with high carbon steel:

The co-efficient of friction of the coating was also analysed with high carbon steel pin at similar loading and sliding conditions, as described in the last cases. The ANOVA was also designed for the response that was co-efficient of friction. The Model F-value of 2033.80 implies the model is significant. Load, sliding speed and their interaction are the significant model terms.

Final Equation in Terms of Coded Factors:

Co-efficient of friction = + 0.81 - 6.810 * 10^{-4} * load - 2.635 * 10^{-3} * load^2 - 0.080 * sliding speed + 4.628 * 10^{-3} * sliding speed^2 - 5.409 * 10^{-5} * load * sliding speed - 6.500 *10^{-3} * load^2 * sliding speed - 1.172 * 10^{-4} * load * sliding speed^2 - 1.911 * 10^{-3} * load^2 * sliding speed^2.

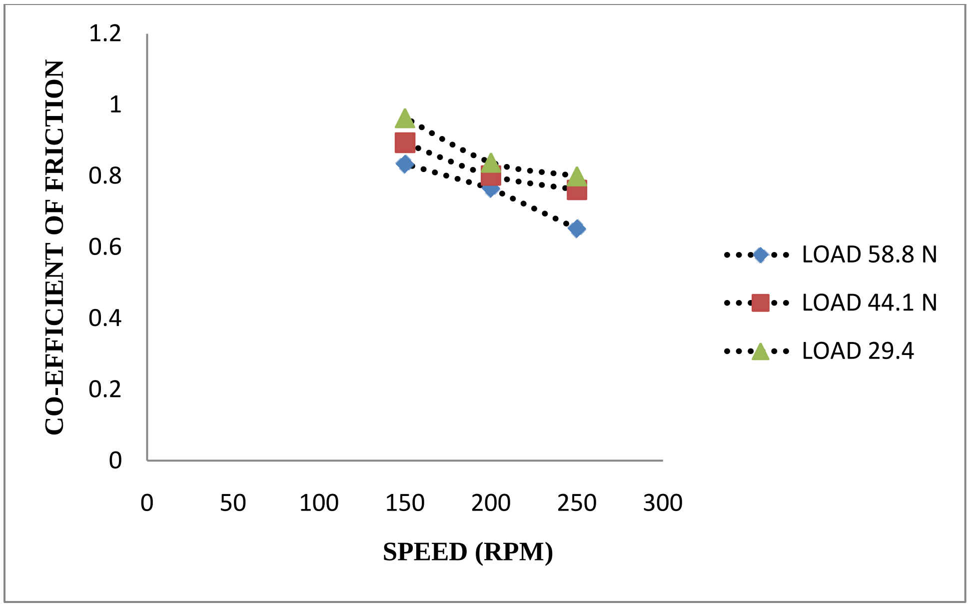

Figure 33. Variation of coefficient of friction with medium carbon steel pin at various loading and sliding conditions

Figure 33 shows the variation of the co-efficient of friction of the coating at different loading and sliding condition. The coefficient of friction of the coating at 29.9 N load and 150 rpm was calculated as 0.9623. The coefficient of friction decreased to 0.8934, at a load of 44.1 N at the same speed. When the load was increased to 58.8 N at the same sliding speed the co-efficient of friction was further decreased to 0.8337. The co-efficient of friction of the coating at 200 rpm speed and 29.9 N load was found to be 0.8378. When the load was increased to 44.1 N at the same sliding speed the co-efficient of friction decreased to 0.8011. It further decreased to 0.7653, when the load was increased to 58.8 at the same sliding speed. The co-efficient of friction at 250 rpm speed and 29.9 N load was 0.7993. It decreased to 0.7606, when the load was increased to 44.1 N at the same sliding speed. It was further decreased to 0.6519, at 58.8 N load and same sliding speed.

The co-efficient of friction of the coating with high carbon steel was more than coefficient of friction with brass and medium carbon steel pin [51,54]. The co-efficient of the friction of the coating was decreased with increase in load [9,12]. The coefficient of friction was also decreased with the increased sliding speed [13,53]. The coating having hardness 58.8 Hv at 5 gm load, it was very less as compared to hardness of the high carbon steel tool pin. So no deformation of the high carbon steel pin was observed during the wear test.

4.4. EDS analysis of worn surfaces:

The EDS analysis of the worn track was carried out on an electric discharge spectrometer at a resolution of 20 µm. Deformed coating layers and metal oxides were observed on the wear track. The wear track of the coating after the wear test at different loadings and sliding conditions with different pin materials like brass, medium carbon and high carbon steel pin were analysed. The EDS results of the coating worn out with brass pin at 150 rpm speed and 58.8 N load is shown in figure 34. At high load and low sliding speeds high deformation and adhesion occurs [56]. During the EDS analysis of the coating some spots of copper and zinc were also found, it may be due to diffusion of the pin over the coating. As the resolution was less, in some EDS tables all the constituents were not recognized.

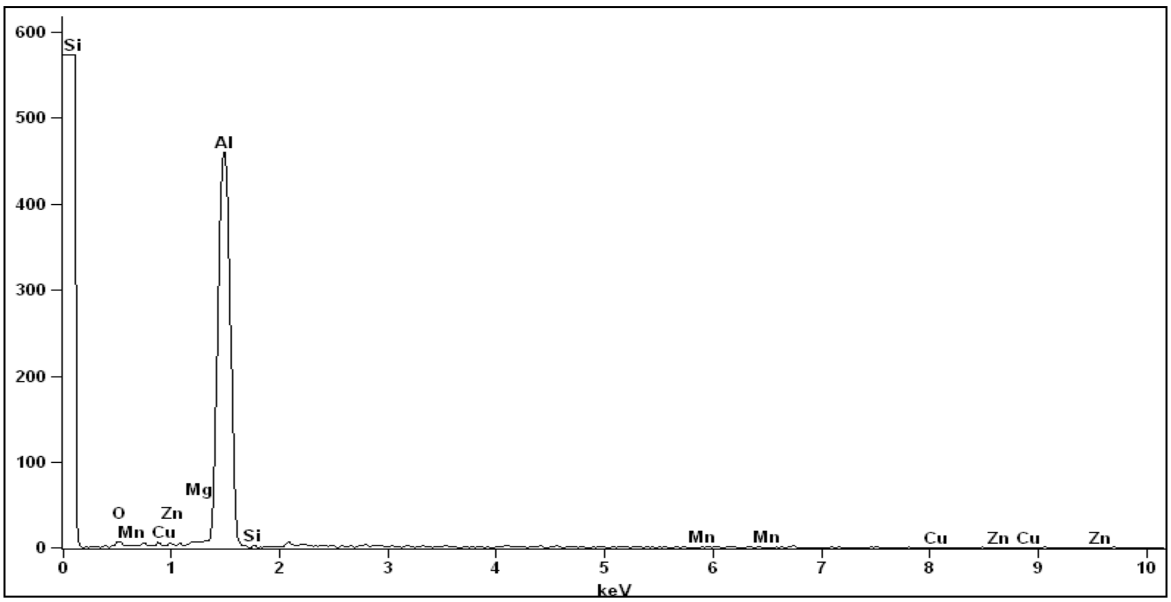

Figure 34. EDS of the worn track of the thermal spray coating 58.8 N load and 150 RPM speed with brass pin

Element Line	Net Counts	ZAF	Weight %	Weight % Error	Atom %	Atom % Error	Compound%
O K	28	2.947	2.47	+/- 0.62	4.09	+/- 1.02	2.47
Mg K	0	0.968	0.00	---	0.00	+/- 0.00	0.00
Al K	5427	1.014	97.53	+/- 1.37	95.91	+/- 1.34	97.53
Si K	0	2.186	0.00	---	0.00	+/- 0.00	0.00
Si L	0	0.000	---	---	---	---	---
Mn K	0	1.189	0.00	---	0.00	+/- 0.00	0.00
Mn L	3	0.000	---	---	---	---	---
Cu K	0	1.217	0.00	---	0.00	+/- 0.00	0.00
Cu L	0	0.000	---	---	---	---	---
Zn K	0	1.222	0.00	---	0.00	+/- 0.00	0.00
Zn L	0	0.000	---	---	---	---	---
Total			100.00		100.00		100.00

Table 4.Quantitative table of EDS analysis of worn surface with brass pin at 150 rpm speed and 58.8 N load

Figure 35 shows the EDS peaks of the coating, worn with medium carbon steel pin load 58.8 N and at a speed of 150 rpm. Aluminum was the major component but some amount of copper, magnesium, manganese, iron, and carbon were also found to be present. During the wear test some pin materials was also diffused over the coating surface so negligible amount of iron and carbon was also transferred on the wear track. Some amount copper and zinc was also found as aluminum impurities.

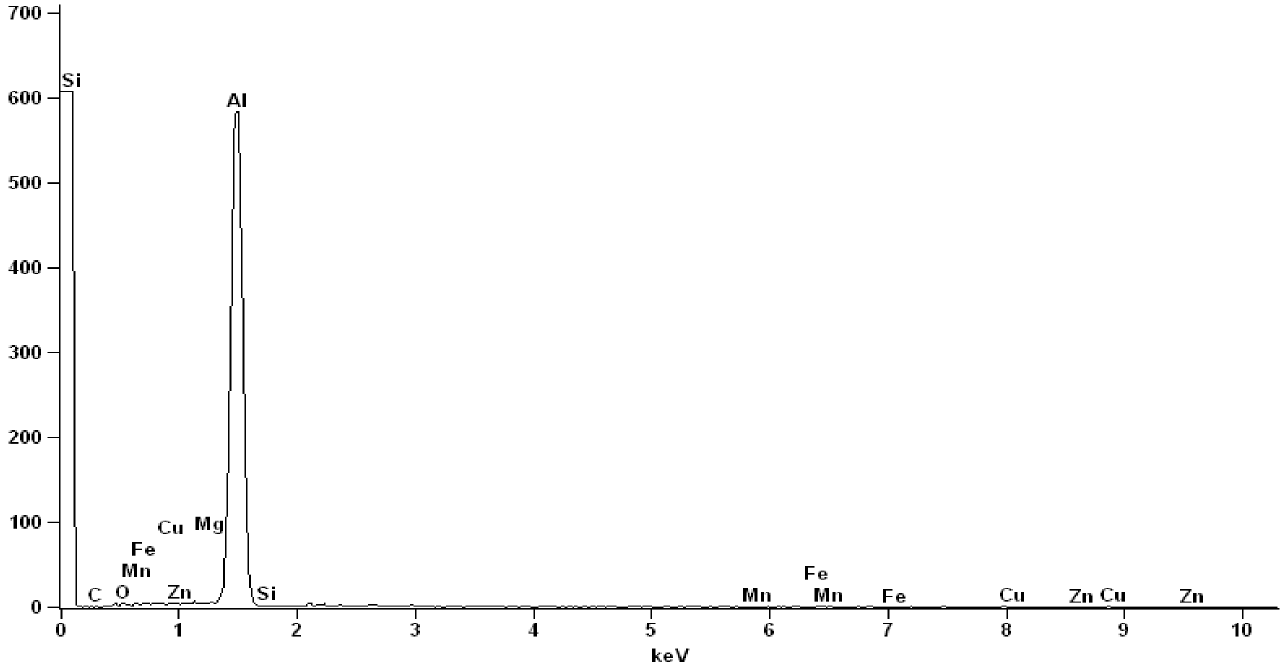

Figure 35. EDS of the worn track of the thermal spray coating 58.8 N load and 150 RPM speed with medium carbon steel pin

Element Line	Net Counts	ZAF	Weight %	Weight % Error	Atom %	Atom % Error	Compound%
C K	4	11.332	0.77	+/- 0.96	1.72	+/- 2.15	0.77
O K	8	2.985	0.58	+/- 0.51	0.97	+/- 0.85	0.58
Mg K	0	0.997	0.00	---	0.00	+/- 0.00	0.00
Al K	6215	1.027	96.60	+/- 1.23	96.35	+/- 1.22	96.60
Si K	0	2.182	0.00	---	0.00	+/- 0.00	0.00
Si L	0	0.000	---	---	---	---	---
Mn K	7	1.185	0.64	+/- 0.55	0.31	+/- 0.27	0.64
Mn L	0	0.000	---	---	---	---	---
Fe K	8	1.162	0.83	+/- 0.83	0.40	+/- 0.40	0.83
Fe L	8	0.000	---	---	---	---	---
Cu K	3	1.215	0.59	+/- 0.98	0.25	+/- 0.42	0.59
Cu L	0	0.000	---	---	---	---	---
Zn K	0	1.218	0.00	---	0.00	+/- 0.00	0.00
Zn L	0	0.000	---	---	---	---	---
Total			100.00		100.00		100.00

Table 5.Quantitative EDS analysis of wear track of thermal spray coating with medium carbon steel pin at 150 rpm and 58.8 N loads

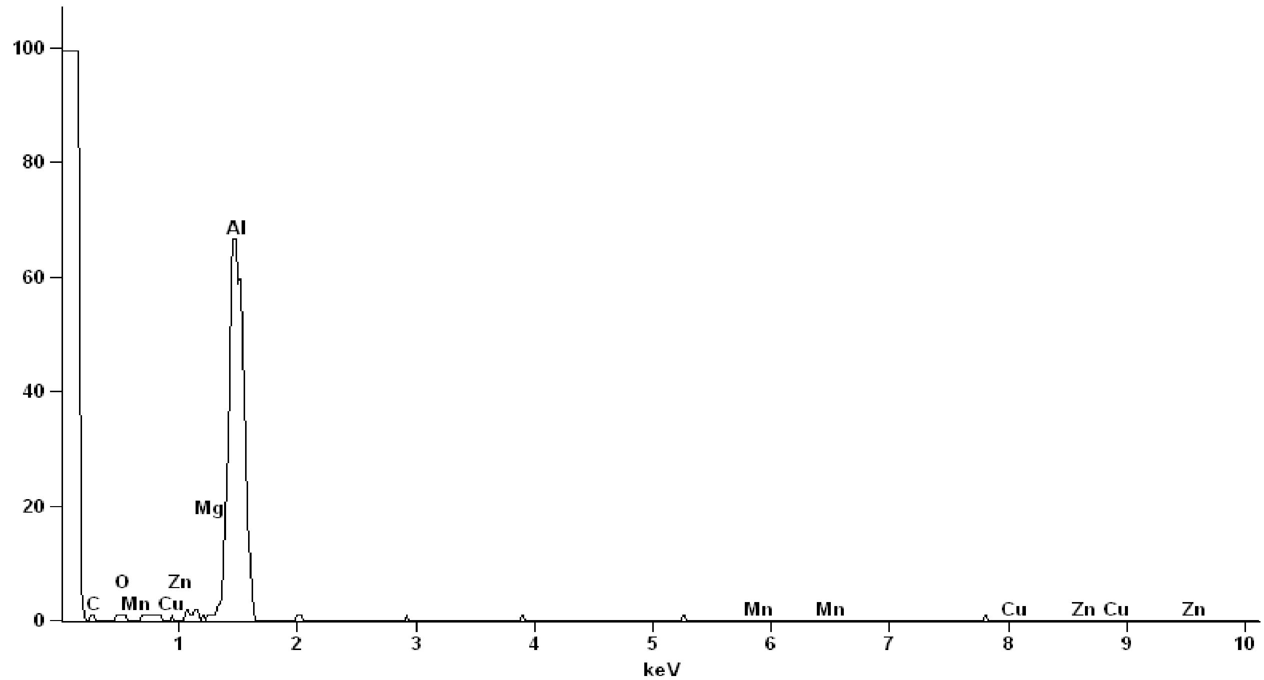

Figure 36. EDS of the worn track of the thermal spray coating 58.8 N load and 150 RPM speed with high carbon steel pin

Element Line	Net Counts	ZAF	Weight %	Weight % Error	Atom %	Atom % Error	Compound%
C K	8	10.404	8.16	+/- 4.08	16.25	+/- 8.12	8.16
O K	9	3.137	3.92	+/- 1.74	5.86	+/- 2.60	3.92
Mg K	0	0.975	0.00	---	0.00	+/- 0.00	0.00
Al K	948	1.045	87.91	+/- 3.52	77.89	+/- 3.12	87.91
Mn K	0	1.191	0.00	---	0.00	+/- 0.00	0.00
Mn L	0	0.000	---	---	---	---	---
Cu K	0	1.219	0.00	---	0.00	+/- 0.00	0.00
Cu L	0	0.000	---	---	---	---	---
Zn K	0	1.225	0.00	---	0.00	+/- 0.00	0.00
Zn L	0	0.000	---	---	---	---	---
Total			100.00		100.00		100.00

Table 6.Quantitative EDS analysis of wear track of thermal spray coating with high carbon steel pin at 150 rpm and 58.8 N loads

Table 6 shows the quantitative table of EDS analysis of the worn surfaces with high carbon steel pin at a load of 58.8 N and sliding speed of 150 rpm. As a result of this analysis, it was found that the aluminum was the major constituent. The pin of high carbon steel was not found to diffuse over the wear track which implies that no iron was present. The presence of oxides of aluminum was more which shows that with high carbon steel the coating material was oxidised to a greater extent. However, with medium carbon steel pin, a significant amount of carbon was found on the wear track. Copper was present as an impurity but no amount zinc was detected.

4.5. Microhardness of the worn surfaces:

The micro hardness of the worn surfaces was determined on Vickers micro hardness tester. The micro hardness of the worn surfaces at the cross section of the worn surface was determined. The micro hardness of the coating was determined at a distance of 0.05 µm from the end of the surfaces. After this the distance taken between the two points of indentation was 1 µm. To determine the micro hardness the work piece was first fixed in a Bakelite cylinder with the help of automatic mounting press (Simplimet 1000, Buehler) at a pressure of 60 psi. The heating time of the thermosetting plastic having sample piece was 12 minutes and cooling times was 3 minutes. After fixing the sample in Bakelite cylinder, it was polished with carbon paper with grit size of 100, 200, and 600. The sample was then polished with aluminum powder paste on polishing machine upto mirror finishing of the sample (surface finish upto 1 µm). The polished sample was put on the job rest of Vickers hardness tester. The load applied over the work piece was 5gm, as aluminum being soft to the indenter will be very large. The time of loading was 10 seconds. The resolution of the indenter was chosen to the 400 X. Upon completion of indentation, the two diagonals were measured, named as D_1 and D_2 (figure 37). The micro hardness of the coating was calculated with the help of these two diagonals.

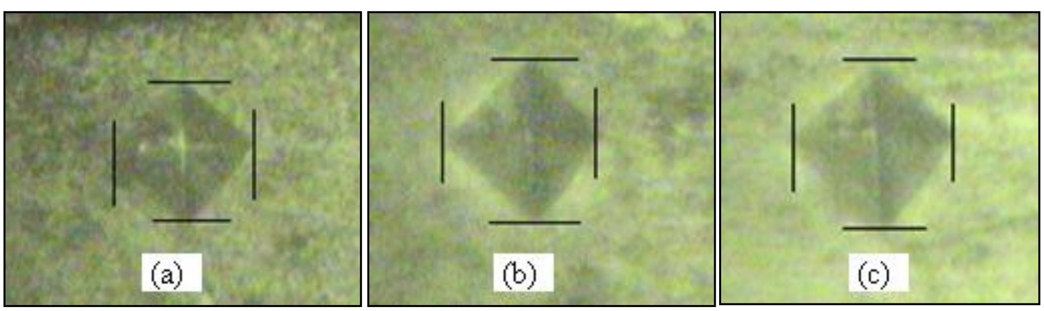

Figure 37. Indentation over the cross section at a distance of 0.05 micro meters from wear track of coating at 250 rpm speed and 58.8 N loads (a) with brass pin (b) with medium carbon steel pin (c) with high carbon steel pin.

4.5.1. Microhardness of the worn surfaces with brass pin:

The micro hardness of the worn surfaces with the brass pin at 58.8N load and 250 rpm sliding speed was determined. Figure 38 shows the variation of Vickers micro hardness, with distance from the cross section of the wear track. The Vickers micro hardness of cross section of the coating at a distance 0.05 µm was 179.31 Hv. The micro hardness of the coating at a distance of 1 µm was 143.66 Hv. It was further reduced to 134.12 at a distance of 2 µm from the cross section of the wear track. The micro hardness of the cross section of the coating at a distance 3 µm and 4 µm was 117.68 and 94.84 Hv.

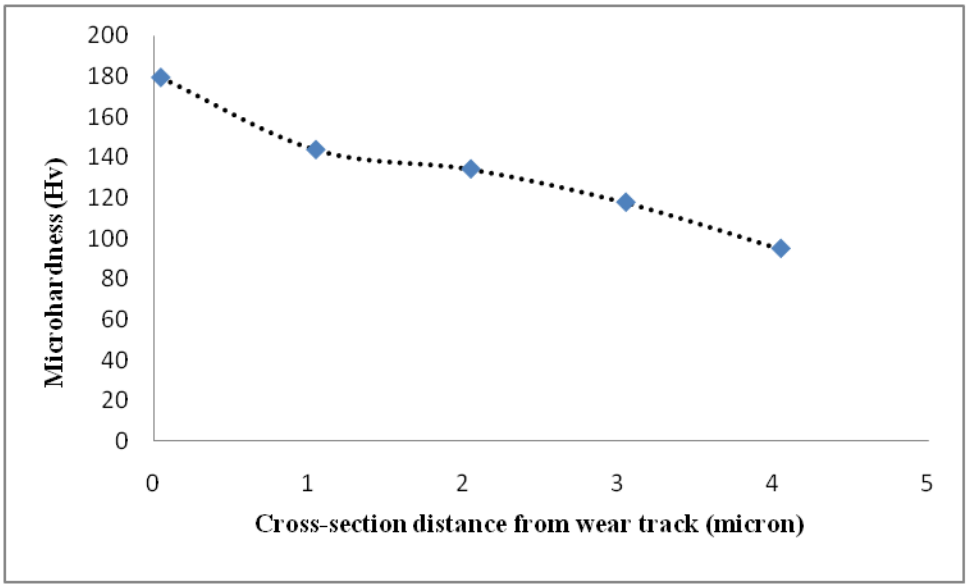

Figure 38. Variation of micro hardness of worn surfaces at cross section distance from wear track with brass pin

The micro hardness of the wear track was decreased away from the wear track. The micro hardness of the worn surface was higher near the wear track due to more deformation and work hardening of the track. The hardening effects were decreased away from the wear track, because the work hardening effects were decreased. The various grade of aluminum and as well as alloy with manganese and magnesium as the major additions, do not respond to strengthening by heat treatment. Approximately 95% of all aluminum flat rolled products (sheet, plate and foil) are made from these three alloy groups. Strength is developed by strain hardening, usually by cold working during fabrication. During deformation of aluminum and its alloys, the dislocations content increases when dislocation generation and multiplication occur faster than annihilation by dynamic theory. Dislocation tangles, cells and sub-grains wall are formed, all of which decrease the mean free slip distance and give increased strength. During deformation, because aluminum has high stacking fault energy, a cellular substructure is formed with in the grain which causes some strengthing. The work hardenability of the aluminum alloy increase with increase of magnesium content [58]. When the pin was slide on the coating surface, strain hardening effects was developed due to force exerted by the pin on the coating surfaces. At higher load high work hardening was observed.

4.5.2. Microhardness of the worn surfaces with medium carbon steel pin:

The micro hardness of the worn surfaces with the medium carbon steel pin at 58.8N load and 250 rpm sliding speed was determined. Figure 39 shows the variation of Vickers micro hardness, with distance from the cross section of the wear track. The Vickers micro hardness of cross section of the coating at a distance 0.05 µm was calculated as 148.65 Hv. The micro hardness of the coating at a distance of 1 µm was 139.52 Hv. It was further reduced to 122.62 at a distance of 2 µm from the cross section of the wear track. The micro hardness of the cross section of the coating at a distance 3 µm and 4 µm were found to be 119.61 and 103.68 Hv.

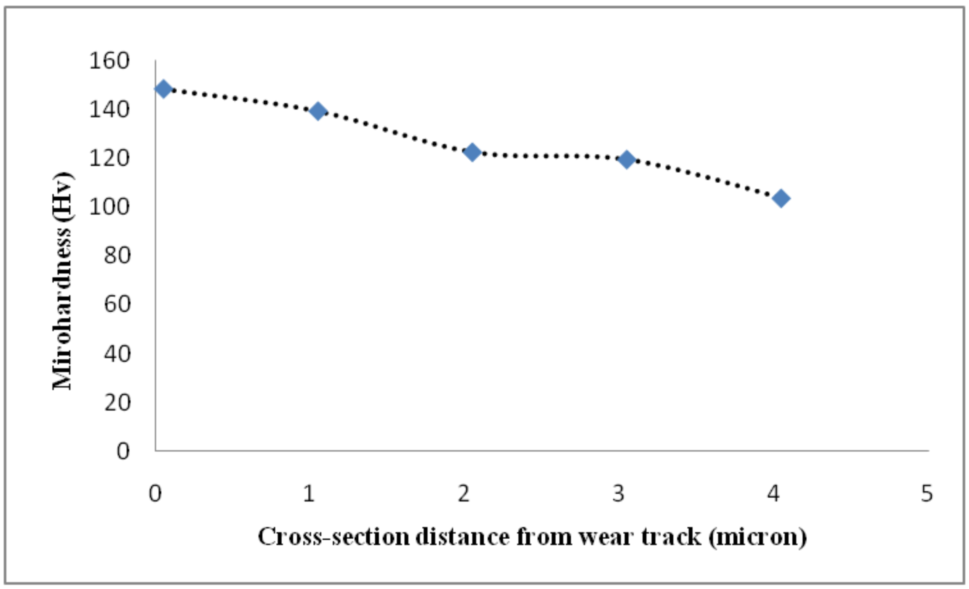

Figure 39. Variation of micro hardness of worn surfaces from cross section with medium carbon steel pin

It was observed that the micro hardness at a distance 0.05 µ (micron) was maximum and then decreased away from the cross section of wear track. The micro hardness of the worn surfaces with medium carbon steel pin was found to be lower than that of micro hardness of the worn surfaces with brass pin may be due the reason that, the coating deformed more and the microcutting was less. It was observed by SEM results that, the main wear mechanism of coating with medium carbon steel pin was mainly due to microcutting and the deformation of the wear track was observed very less. As deformation was very less, so strain hardening effects was found to be very less. The deformation effects were uniform so that the variation of the micro hardness was also very less.

4.5.3. Microhardness of the worn surfaces with high carbon steel pin:

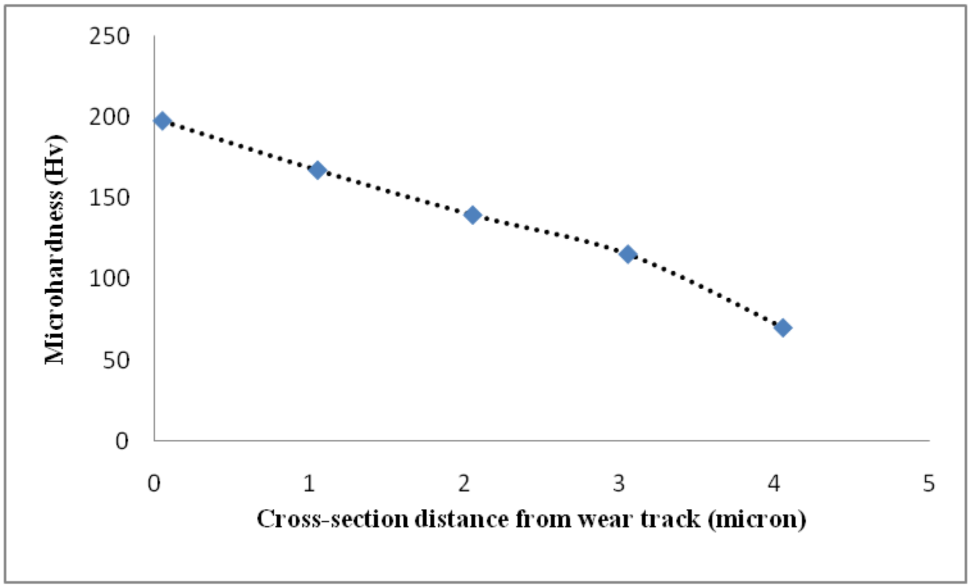

Figure 40. Variation of micro hardness of worn surfaces from cross section with high carbon steel pin

The micro hardness of the worn surfaces with the medium carbon steel pin at 58.8N load and 250 rpm sliding speed was determined. Figure 40 shows the variation of Vickers micro hardness, with distance from the cross section of the wear track. The Vickers micro hardness of cross section of the coating at a distance 0.05 µm was found to be197.73 Hv. The micro hardness of the coating at a distance of 1 µm was 167.25 Hv. It was further reduced to 139.52 at a distance of 2 µm from the cross section of the wear track. The micro hardness of the cross section of the coating at a distance 3 µm and 4 µm was 115.3 and 69.85 Hv.

The micro hardness of the cross section of worn surface with high carbon steel pin near the wear track was found to be more than that the worn surface of the coating with brass and medium carbon steel. However, away from the cross section of the wear track the micro hardness decreased at a faster rate. The micro hardness near the wear track was very high that was 197.93 Hv but at a distance 4 µ (micron) the hardness was only 69.85. It was may be due to the reason that the wear mechanism in case of high carbon steel pin is mainly due to micro cutting and the deformation is only on the wear track whereas, the work hardening was only over the wear track, below which the work hardening effects were very less.

4.6. Microstructure of worn surfaces of the coating:

The microstructure of the coating was studied under the optical microscope. To study the microstructure a piece of the track of coating was cut and then fixed in the thermosetting plastic to hold it. The fixing of the small piece of the coating piece was done on the automatic mounting press as described earlier in micro hardness test. The cross section of worn surfaces was analyzed, when the pin was sliding over the coating material there was a generation of heat which might result in change in the microstructure. It is known that the melting point of the aluminum is 662˚C [1] and when there is rise in temperature above recrystalisation temperature then there occurs a change in the microstructure. The aluminum is a good conductor of heat so heat generated during the wear test is rejected to the surrounding [4].

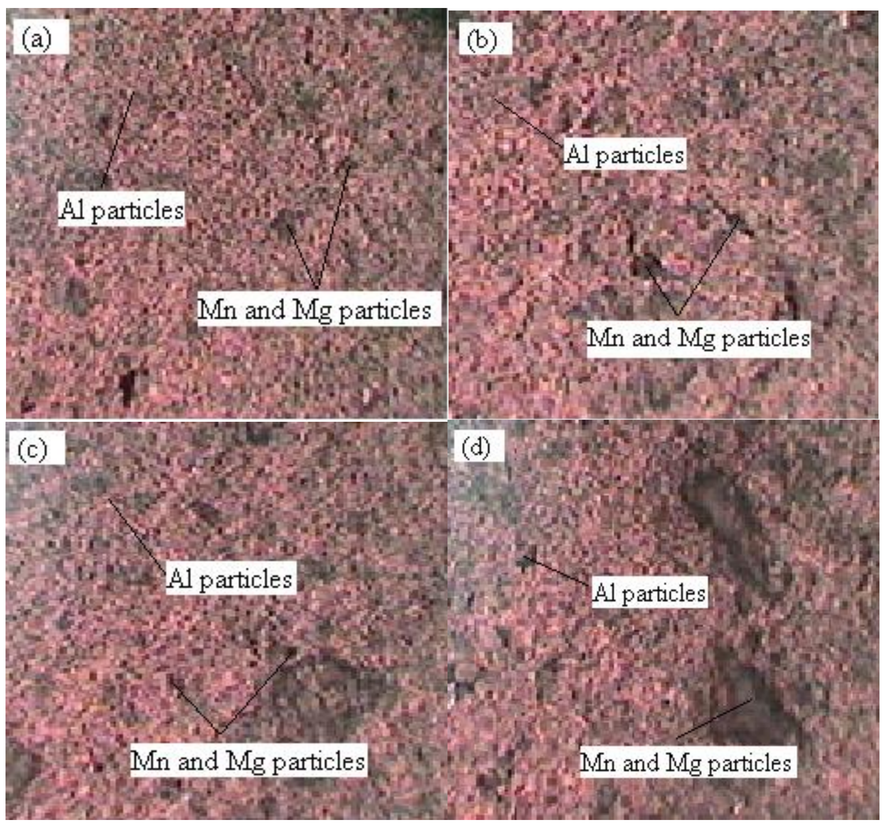

Figure 41. Micro structure of the cross section of the worn surfaces. (a)Aluminum alloy coating (b) at 29.4 N load (c) at 44.1 N load (d) at 58.8 N load

Figure 41(a) shows the microstructure of the cross section of the coating before wear test. It was compared with the microstructure of the coating after the wear test. The microstructure of the wear track of the coating at three different loads 29.4, 44.1 and 58.8 N was observed and it was found that there is no significant change in the microstructure (figure 41b, 41c, 41d). The microstructure of cross section of the coating was found to be similar before and after the wear test. With these results it may be concluded that wear was not accompanied by melting of coating surfaces and that the main wear mechanism was only due to deformation, adhesion, and cutting.

4.7 XRD analysis of worn surfaces of the coating:

As the wear occurs of the coating then there should be decrease in the d-spacing of the crystal. If the stress is non uniform, different crystal or different parts of the same crystal may be deform to differing degrees and the crystal line become broadened [57]. Stress in the coating may be caused by application of external load. And stress may also cause by internally due to consequence of the deformation takes place inside the crystal.

The value of d spacing of coating at the wear track at a load of 29.4 N and 250 rpm sliding speed with brass pin was found to be 3.69634 Ǻ (figure 42). When the load was increased to 44.1 N, the value of d spacing was found to be 2.34347 Ǻ. It showed that the value of d spacing was decreased with increased in the load. The value of the ‘θ’ was found to be increased with the increased load. Initially the value of 2θ was found to be 38.380˚ at 250 rpm speed and 29.4 N load. When the load was increased to 44.1 N the value of 2θ was found to be 38.4494˚. It was found to be further increased to 38.5690 at 58.8 N load and the same sliding speed. The peaks of XRD were found to be shifted towards right hand side with increased load. It was clear from these observations that the deformation of the wear track of the coating was increased with the increased load. It was also observed that when the sliding speed was decreased the value of d spacing was found to be decreased; it may be due to reason that at lower speed the deformation of the crystals was more.

The XRD peaks obtained for the wear track of coating with medium carbon steel pin and high carbon steel pin were almost same. In the case of wear of coating with high carbon steel and medium carbon steel pin, the wear mechanism was not due to deformation, but due to micro cutting. At low load some shear force might have come into play, but at higher load the wear was mainly due to abrasion and micro cutting.

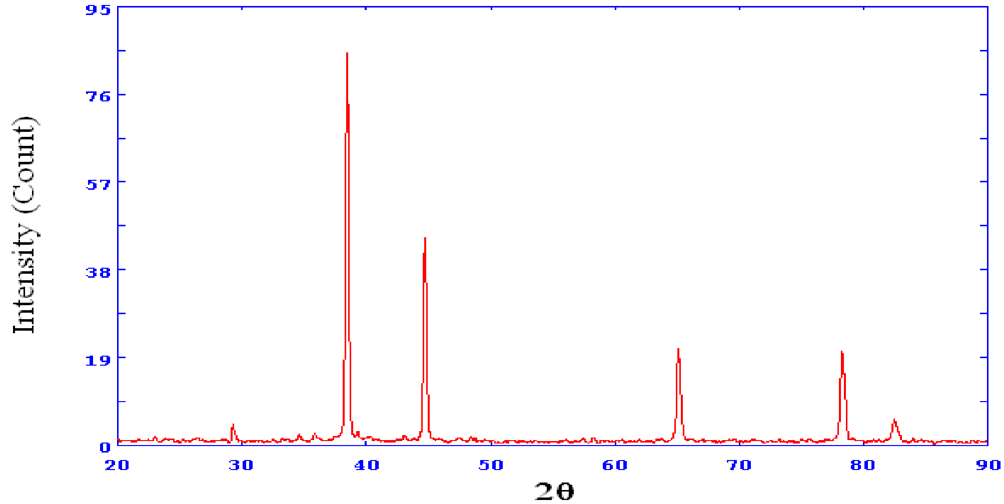

Figure 42. XRD peaks with brass pin at 250 rpm speed and 29.4 N loads

The value of d spacing of the coating worn with medium carbon steel at a load of 29.4 N load and 250 rpm speed was found to be 3.68879 A˚ (figure 43). It was found to be decreased to 3.67745 A˚ at a load 58.8 N load under similar sliding speed. The value of d spacing of the worn surfaces of the coating with high carbon steel at a load of 29.9 N and 250 rpm speed was found to be 3.69145 A˚ (figure 44). It was found to be decreased to 3.69028 A˚ at a load of 44.1 N load and 250 rpm sliding speed.

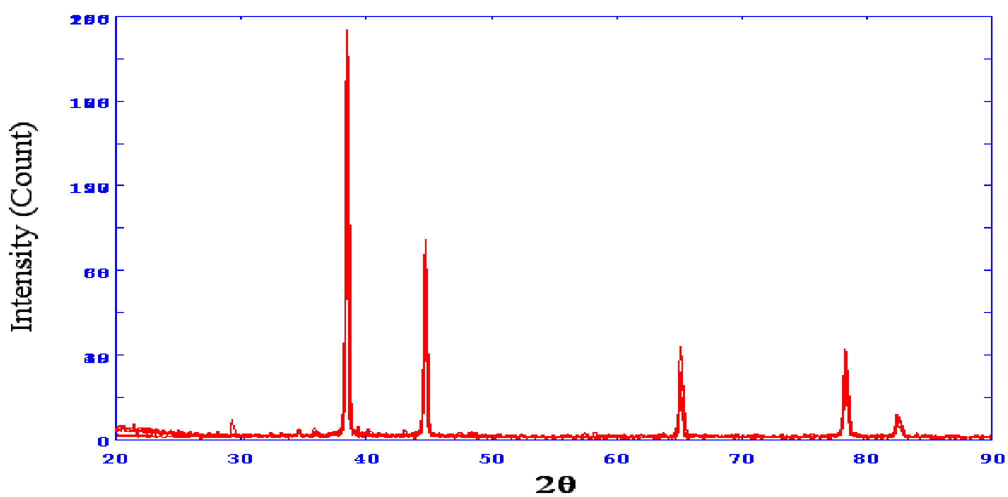

Figure 43. XRD peaks with medium carbon steel pin at 29.4 N load and 250 rpm speed.

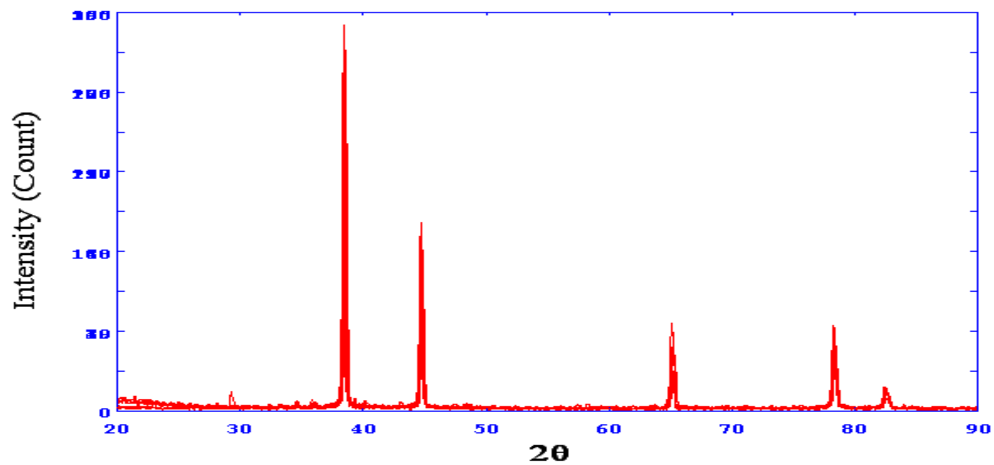

Figure 44. XRD peaks with high carbon steel pin at 3 kg load and 250 rpm speed

When the load was increased to 58.8 N, the value of d was found to be decreased to 3.67745 A˚. From these observations it was concluded that that the value of d spacing was decreased with increased load. The decrease in the d spacing at increased load was due to reason that at high load the coating crystals were deformed more and the intermolecular space between the two atoms were decreased. The value of d spacing of the worn surfaces with brass pin was found to be more; it may be due to reason that the brass pin was less hard as compared to medium carbon and high carbon steel pin, so the coating surface was more deformed with brass pin. Due to this deformation the particles of the coating were come closer to each other which may decrease the value of d spacing. However in wear track of the coating with medium carbon and high carbon steel the deformation was very less and micro cutting was more so the value of d spacing was found to be high.

4.8 Wear mechanism:

4.8.1 Wear mechanism with brass pin:

In order to study the wear mechanism the worn surface were examined by scanning electron microscope. The scanning electron microscope gives the 3D surface morphology of the wear track which helps in the interpretation of the wear mechanism at various loading conditions and various speeds.

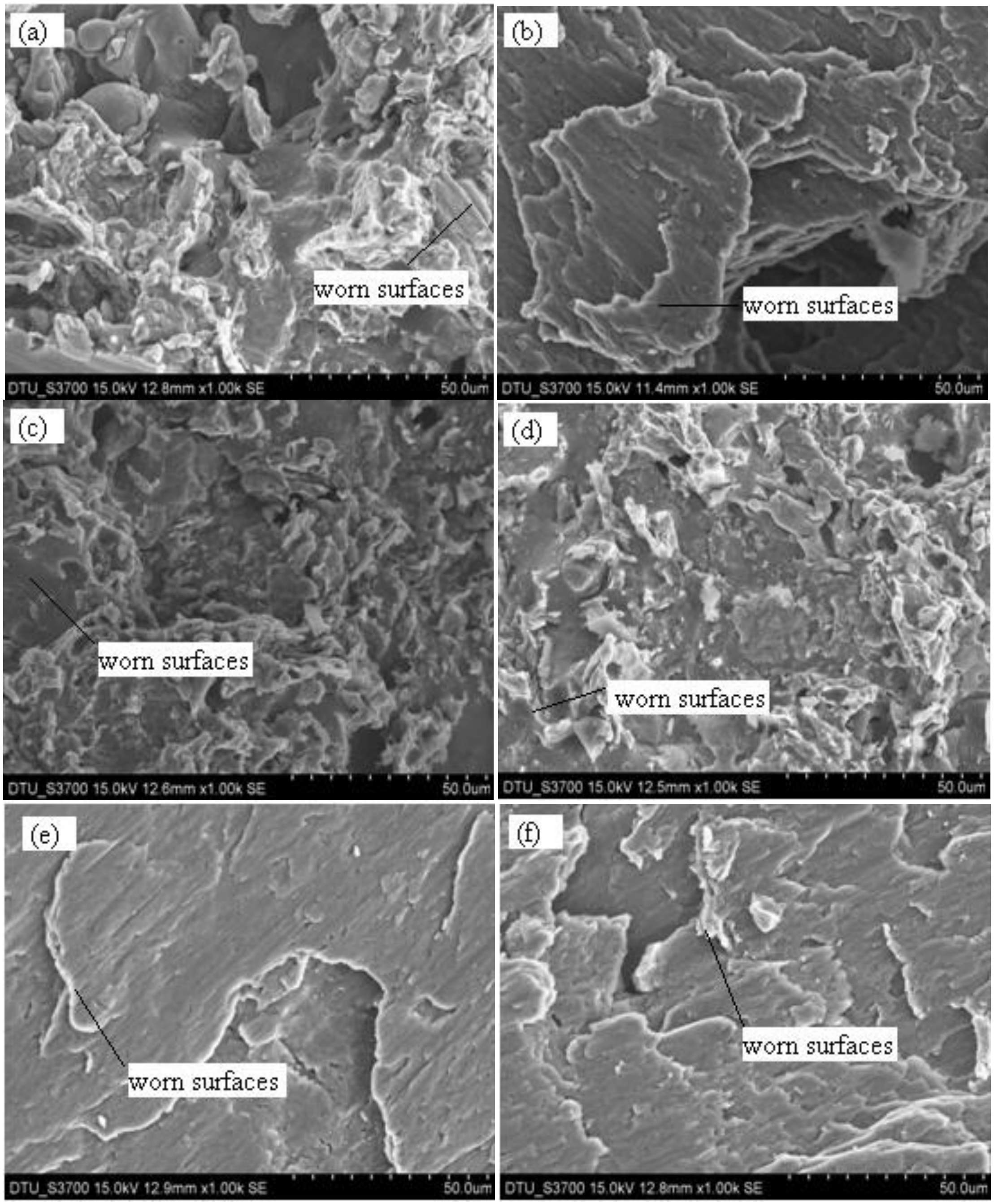

Figure 45. (1)Worn surface with brass pin, at 250 rpm speed and (a) 29.4 N load (b) 44.1 N load (c) 58.8 N load. (2) At 200 rpm speed and (d) 29.4 N loads (e) 44.1 N load (f) 58.8 N loads.

The wear mechanism of the thermal spray coating with brass pin, at 29.4 N load and 250 rpm speed was analysed and it was found that the wear mechanism was mainly due to micro cutting and abrasion (figure 45a). When the load was increased to 44.1 N at the same 250 rpm speed then adhesion also seems to come into picture. Due to this adhesion some deformation was also observed (figure 45b). The deformed particles get flattened over the coating surface. With an increased load 58.8 N and the same 250 rpm speed, long worn debris was generated. At higher loads and sliding speeds the occurrences of severe metallic wear by physical metallic failure are more dominating [4]. Due to this deformation was less and the micro cuttings were more (figure 45c). At 200 rpm and the load of 29.4 N the wear was very less, because the pin just slides over the coating material and the adhesion was very less. The main wear mechanism was only due to erosion of the coating (figure 45d). When the load was increased to 44.1 N, the wear mechanism of the coating was also included adhesion wear as with the micro cutting. So there was deformation of the coating material and some amount of the copper also gets adhered over the wear track (figure 45e). The coating at 44.1 N loads deformed and gets flattened over the wear track. At the 58.8 N loads and the same 200 rpm it was found that the adhesion was more and the coating material got more deformed and more flattened over the wear track (figure 45f).

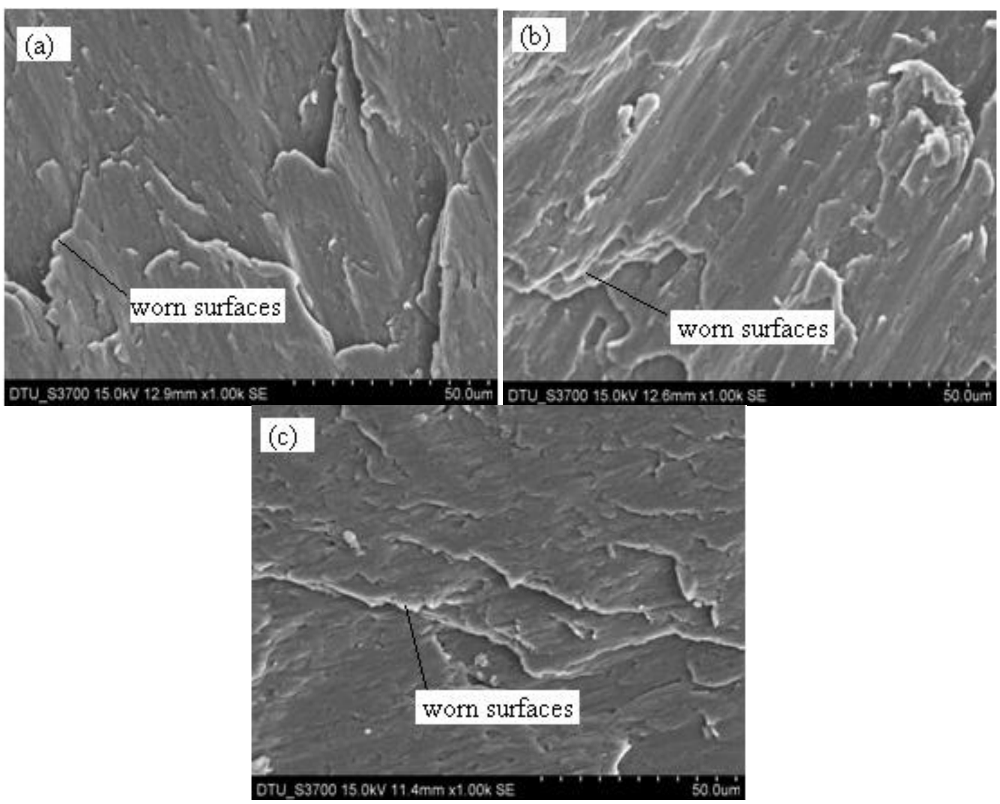

Figure 46. Worn surface with brass pin, at 150 rpm speed and (a) 29.4 N load (b) 44.1 N load (c) 58.8 N load

The wear mechanism of the coating was also analysed with 150 rpm speed and 29.4 N load some deformation was found to take place (figure 46a). As the load was increased to 44.1 N the deformation of the worn surface was more. The worn surfaces were found to be more adhered to the coating surface hence, the wear mechanism was found in case of 44.1 N load mainly due to delaminating and adhesion (figure 46b). When we increased the load to 58.8 N over the same speed of the disc, then the adhesion of the coating over the wear track was found to be more (figure 46c). Shunyan Tao et al. [56], has also previously reported that the deformation of the coating with copper pin at high load and low speed was more.

4.8.2 Wear mechanism with medium carbon steel:

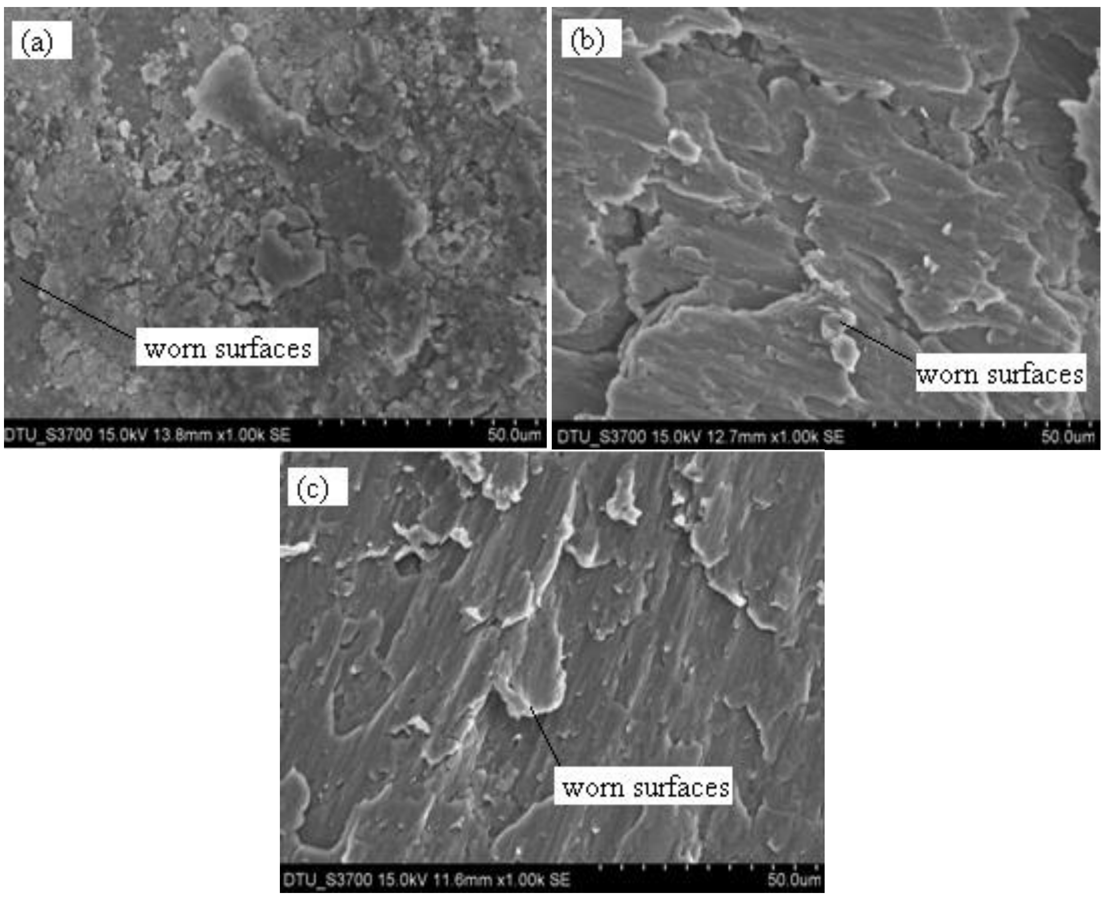

Figure 47. Worn surfaces with medium carbon steel at 250 rpm speed and (a) 29.4 N load (b) 44.1 N load (c) 58.8 N load

When the medium carbon brass pin slided over the coating at 250 rpm speed and 29.4 N load then abrasion of the coating was more and the wear debris was in the form of microchips (figure 47a). These microchips were suddenly removed over the track due to high velocity. At 44.1 N load and 250 rpm speed deformation was found to be more, due to high pressure exerted by the pin. The worn debris also got deposited over the wear track (figure 47b). When the wear load was further increased to 58.8 N, there was more deformation of the coating surfaces (figure 47c). With brass pin the pin material got deformed and the diffusion observed was more, whereas in case of medium carbon steel pin the pin did not get deformed.

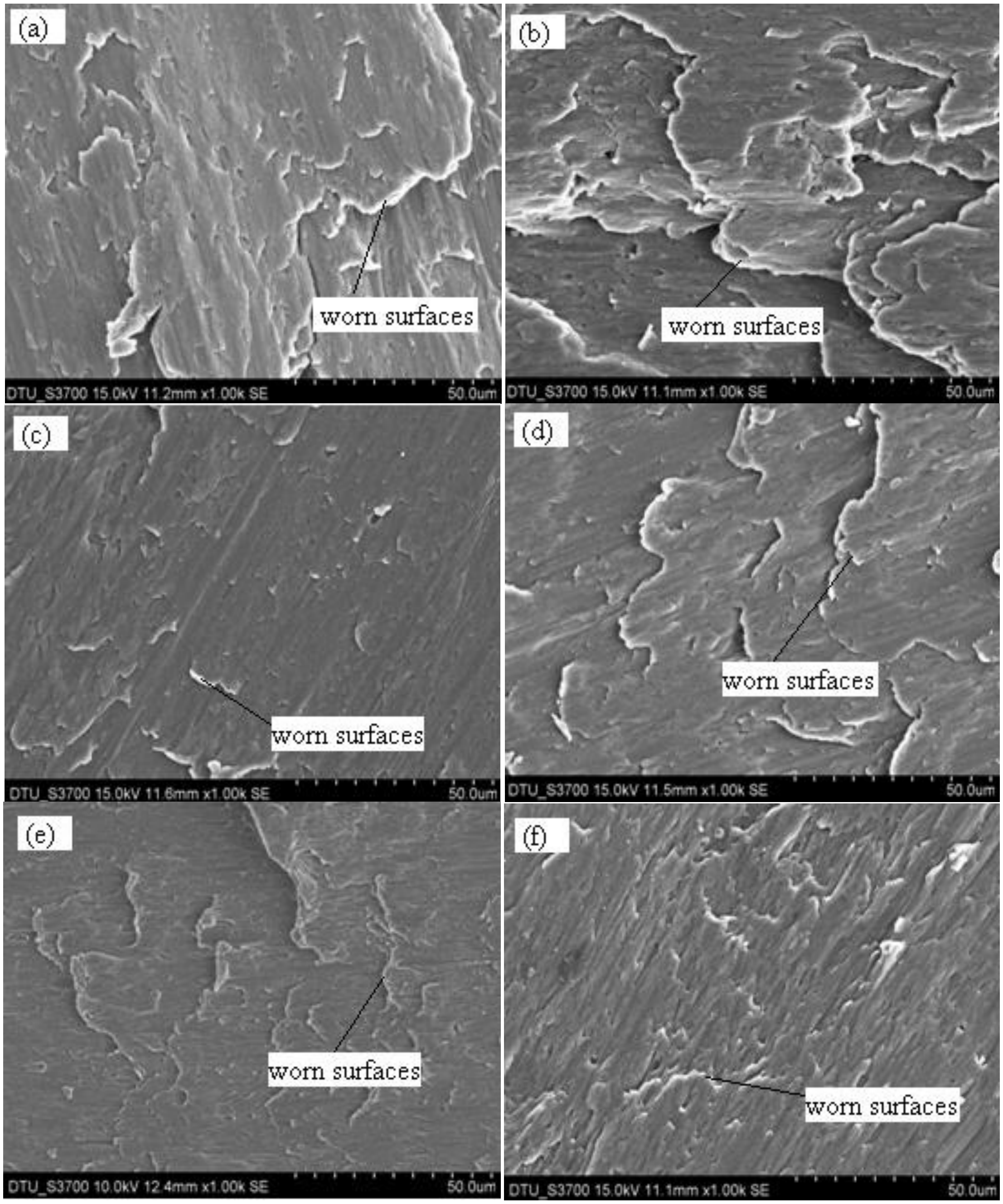

Figure 48. (1)Worn surface with medium carbon steel pin, at 200 rpm speed and (a) 29.4 N load (b) 44.1 N load (c) 58.8 N load. (2) At 150 rpm speed and (d) 29.4 N loads (e) 44.1 N load (f) 58.8 N loads

When the speed of the disc was decreased to 200 rpm then there was more deposition than in case of 250 rpm speed. At this speed the wear behaviour was not only due to abrasion but also due to deformation, the coating surfaces get deformed and adhered over the surface. At a load of 29.9 N load and 200 rpm deformations were less and micro cutting was the major wear mechanism (figure 48a). If the load was increased to 44.1 N at the same speed, the deformation of the coating was more (figure 48b). At 58.8 N loads and 200 rpm speed, the coating got deformed and deposited over the coating surface forming a thin layer hence the surface was found smooth (figure 48c). Slow speed caused more plastic deformation of the coating material and the abrasion of the coating was less. The wear behaviour at 150 rpm speed and a load of 29.4 N was also studied and it was found that at this load, the shear of the coating was more and the coating was more deformed due to slow speed (figure 48d). When the load was further increased to 44.1 N over the pin then the shear observed was more and the plastic deformation of the coating was high (figure 48e). At higher load of 58.8 N the wear rate of the coating increased, the micro cutting of the coating was high and the deformation of the coating was less (figure 48f).

4.8.3. Wear mechanism with high carbon steel:

The wear mechanism of the aluminum alloy coating with high carbon steel was analyzed at same sliding and loading condition as in the case of brass and medium carbon steel pin. The wear mechanism at 250 rpm speed and 29.4 N load having very less deformed surfaces and the worn debris was observed in the form of micro chips (figure 49a). At the loads of 44.1 N and at the same sliding speed, some deformation of the surfaces was observed but the main wear mechanism was due to abrasion and micro cutting, some amount of plastic deformation was also present over the wear track (figure 49b). When the load was further increased to 58.8 N at the same sliding speed, the deformation of the wear track was more and the wear was also in the form of micro cutting (figure 49c). The high carbon steel is harder as compared to brass pin and medium carbon steel so the deformation of the wear track was very less and the main wear mechanism observed was micro cutting.

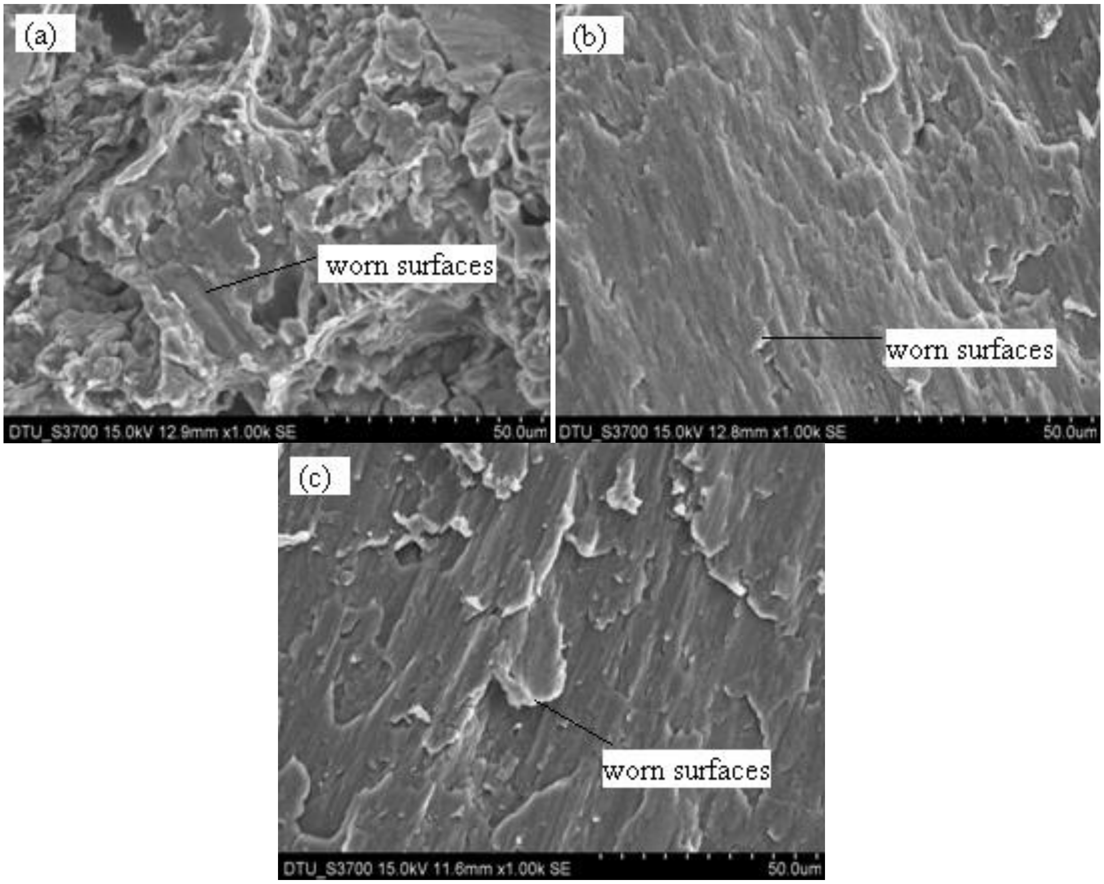

Figure 49. Worn surfaces with high carbon steel at 250 rpm speed and (a) 29.4 N load (b) 44.1 N load (c) 58.8 N load

At 200 rpm speed and 29.4 N load the deformation was high as compared to deformation in case of 250 rpm speed at same 29.4 N load (figure 50a). When the load was increased to 44.1 N at the same 200 rpm speed the deformation as well as micro cuttings were also increased (figure 50b). At 58.8 N load and 200 rpm speed deformation was much higher along with the micro cutting and abrasion (figure 50c).

At 150 rpm speed and 29.4 N load the deformation as well as micro cutting was less, along with less deformation of the wear track (figure 50d). At the same speed and load of 44.1 N the deformation of the coating was more pronounced together with the micro cutting of the coating, but less than that at high speed (figure 50e). When the load was increased to 58.8 N, the wear track surface got more deformed along with more micro cutting and worn debris (figure 50f). However, it was found that with decreased speed the deformation of the coating surface was more while the micro cuttings were very less.

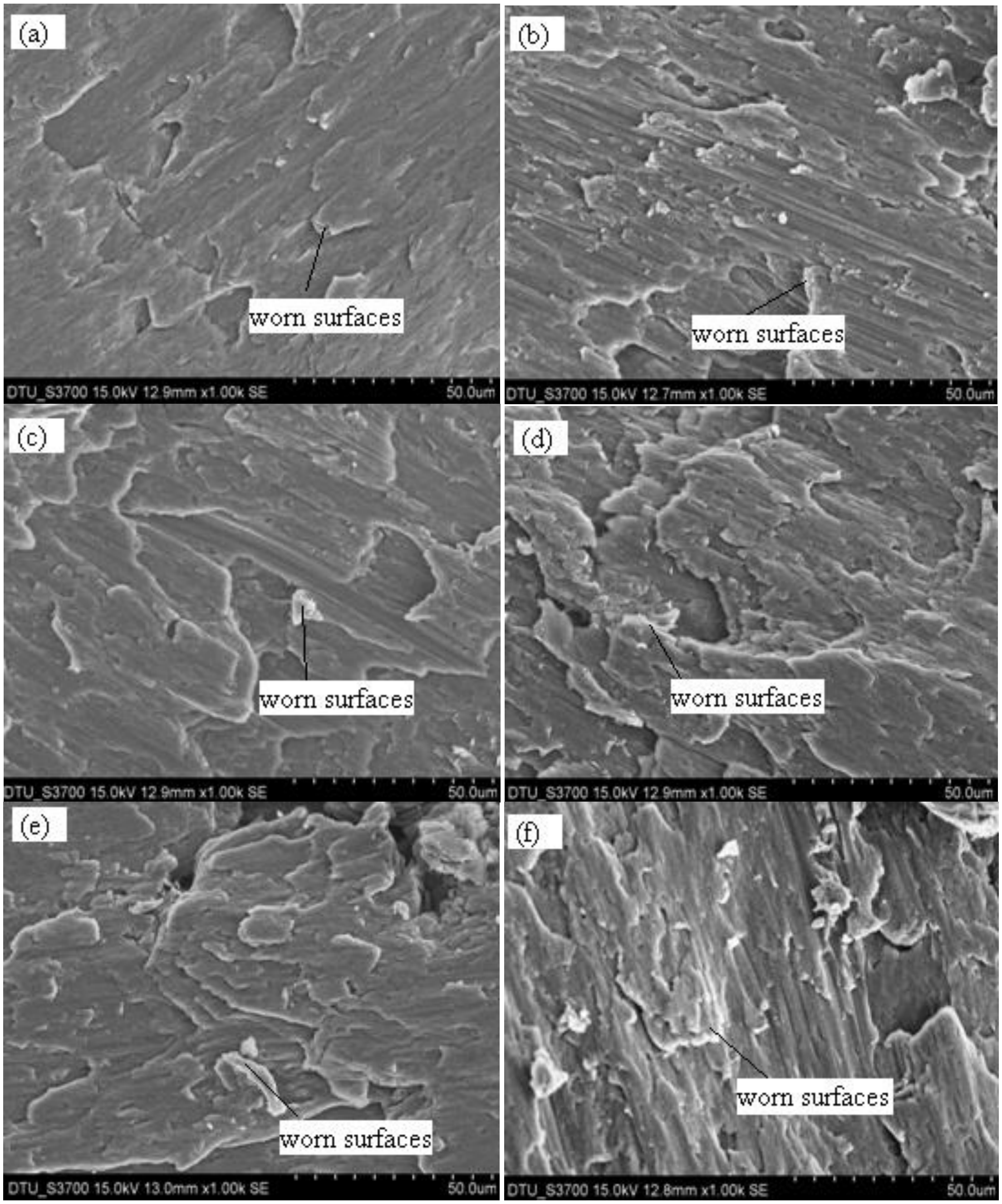

Figure 50. Worn surface with high carbon steel pin, at150 rpm speed and (a) 29.4 N load (b) 44.1 N load (c) 58.8 N load. (2) At 150 rpm speed and (d) 29.4 N loads (e) 44.1 N load (f) 58.8 N loads.